

Finite Size Effect in the Quantum Anomalous Hall system

Hua-Hua Fu,* Jing-Tao Lü, and Jin-Hua Gao†

*College of Physics and Wuhan National High Magnetic field center,
Huazhong University of Science and Technology, Wuhan 430074, China.*

(Dated: March 14, 2014)

We theoretically investigate the finite size effect in quantum anomalous Hall (QAH) system. Using Mn-doped HgTe quantum well as an example, we demonstrate that the coupling between the edge states is spin dependent, and is related not only to the distance between the edges but also to the doping concentration. Thus, with proper tuning of the two, we can get four kinds of transport regimes: quantum spin Hall regime, QAH regime, edge conducting regime, and normal insulator regime. These transport regimes have distinguishing edge conducting properties while the bulk is insulating. Our results give a general picture of the finite size effect in QAH system, and are important for the transport experiments in QAH nanomaterials as well as future device applications.

PACS numbers: 73.43.-f, 72.25.Dc, 85.75.-d, 75.50.Pp

Quantum anomalous Hall (QAH) state is a new state of matter of two dimensional (2D) insulator, which has a quantized Hall conductivity without Landau level.¹⁻⁴ Energy band of the QAH state is topological nontrivial and can be characterized by the first Chern number, similar to the quantum Hall state.^{5,6} Different from the normal quantum hall state, the QAH state does not need an external magnetic field to break the time reversal symmetry (TRS).⁷⁻¹⁰ Haldane proposed the first model of QAH state on honeycomb lattice in 1988.¹¹ Stimulated by the discovery of topological insulator (TI),¹² there has been extensive effort to find QAH state in realistic materials, based on theoretical proposals, e.g., mercury-based quantum wells,⁵ disorder induced Anderson insulators,⁶ graphene system,^{13,14} silicene,¹⁵ and magnetic topological insulators.¹⁰ This has led to its recent experimental observation in magnetic TI of Cr-doped (Bi,Sb)₂Te₃.¹⁶ Numerous exotic properties of the QAH state are yet to be explored, which are not only of fundamental importance but also have potential applications.

In this work, we theoretically investigate the QAH system in a finite stripe geometry, where the finite size effect can influence its transport property. The same effect in quantum spin Hall (QSH) system,¹⁷ as well as in the 3D topological insulators,^{18,19} has been studied in details in last few years. A key finding is that, when the sample is narrow enough, the coupling of edge states will open an energy gap, and the quantized conductance of the edge states disappears. Thus, there exists a critical width in QSH system, below which the gapless edge states are destroyed. The finite size effect is crucial for the device application, since it determines the transport property of small device. Here, we illustrate that the finite size effect in the QAH system is more complex than that in QSH system. Due to the magnetic doping, the coupling between edge states becomes spin dependent, and is also related to the doping concentration. Given the width of ribbon and the doping concentration, we can distinguish four kinds of transport regimes in a QAH ribbon. While the bulk is insulating in all these transport regimes, they have different edge conducting behaviors. Because that

the edge conducting channel is the key feature of topological nontrivial system and is the base of many novel quantum electronic devices, our results may be important for the QAH state in nanomaterials as well as the device application of the QAH system.

The system we study is a Mn-doped HgTe quantum well (QW). Without Mn doping, its electronic states can be described by an effective four band model. QSH effect occurs at certain well thickness.²⁰ Note that HgTe QW is the first experimentally confirmed QSH system,²¹ where the finite size effect is well understood and is much more obvious than that in other TI materials.¹⁷ Therefore, it is an ideal example to start with, and it will be easier to compare the finite size effect of QAH with that of QSH system. But we emphasize here that our results are not just limited to the HgMnTe system. They actually offer a general picture for the finite size effect of the QAH state in magnetic doped TI systems.

As a starting point, we introduce the effective Hamiltonian of the HgTe QW. The HgTe QW has an inverted band structure, where the *p*-type Γ_8 has higher energy compared to the *s*-type Γ_6 band at the Γ point. The QSH phase appears as the QW thickness crosses over a critical value.²⁰ The HgTe QW can be described by an effective four-band model⁵

$$H_0(k) = \begin{pmatrix} h_+(\mathbf{k}) & 0 \\ 0 & h_-(\mathbf{k}) \end{pmatrix}, \quad (1)$$

with the basis of $\{|E_1, \frac{1}{2}\rangle, |H_1, \frac{3}{2}\rangle, |E_1, -\frac{1}{2}\rangle, |H_1, -\frac{3}{2}\rangle\}$. $h_+(\mathbf{k}) = M_1(\mathbf{k}_x\sigma_x - \mathbf{k}_y\sigma_y) + (M_0 + M_2\mathbf{k} \cdot \mathbf{k})\sigma_z + \epsilon_{\mathbf{k}}$ where $\sigma_{x,y,z}$ are Pauli matrix. $h_-(\mathbf{k}) = h_+^*(-\mathbf{k})$ is required by TRS, and $\epsilon_{\mathbf{k}} = C_0 + C_2k^2$. The parameters M_0 , C_0 , C_2 , M_1 and M_2 depend on the thickness of the quantum well and the materials details, which can be obtained in Refs. 22 and 23. $h_{\pm}(k)$ is actually equivalent to two dimensional Dirac model, which has a quantized Hall conductance $\pm e^2/h$. Thus, the net Hall conductance of the HgTe QW is zero but the spin Hall conductance is nonzero. The QSH state can be viewed as two copies of QAH states with opposite Hall conductance. For numerical calculation, the tight-binding representation of the

four-band Hamiltonian on square lattice is used.^{24–26}

To realize the QAH phase, magnetic doping is needed to break the TRS between the two spin blocks. When one spin block is in normal insulating regime, but the other is topological nontrivial, QAH state appears, resulting in nonzero net Hall conductance. The spin splitting induced by the magnetization of the Mn atoms is described by a phenomenological term

$$H_s = \begin{pmatrix} G_E & 0 & 0 & 0 \\ 0 & G_H & 0 & 0 \\ 0 & 0 & -G_E & 0 \\ 0 & 0 & 0 & -G_H \end{pmatrix}, \quad (2)$$

e.g., $2G_E$ for the $|E_1, \pm\frac{1}{2}\rangle$ band and $2G_H$ for the $|H_1, \pm\frac{3}{2}\rangle$ band. Thus the energy gap is given by $\Delta E_\uparrow = 2M_0 + G_E - G_H$ for the up-spin block, $\Delta E_\downarrow = 2M_0 - G_E + G_H$ for the down-spin block. The QAH phase in the $\text{Hg}_{1-y}\text{Mn}_y\text{Te}$ QW has been discussed in detail in Ref. 5, and here we just give a short summary. In order to achieve the QAH phase in the $\text{Hg}_{1-y}\text{Mn}_y\text{Te}$ QW, a key relation $G_E G_H < 0$ is required. The expressions of G_E and G_H are $G_E = -(3AF_1 + BF_4)$ and $G_H = -3B$, where F_1 (F_4) is the amplitude of Γ_6 (Γ_8) component in the states $|E_1, \pm\frac{1}{2}\rangle$, $A = \frac{1}{6}N_0\alpha y\langle S\rangle$ and $B = \frac{1}{6}N_0\beta y\langle S\rangle$.^{27,28} N_0 is the number of unit cells per unit volume. α and β describe $sp-d$ exchange coupling strength for the s -band and the p -band electron. For $\text{Hg}_{1-y}\text{Mn}_y\text{Te}$, the parameters are $F_1 = 0.57$, $F_4 = 0.43$, $N_0\alpha = 0.4$ eV and $N_0\beta = -0.6$ eV. The Mn doping is described by two parameters, i.e. doping concentration y and the single Mn atom spin polarization out of QW plane $\langle S\rangle$. With proper doping parameters, e.g. $y=0.02$ and $\langle S\rangle = 2$, we can get QAH phase in this system.

Our goal is to explore the finite size effect in the QAH system, so we investigate the $\text{Hg}_{1-y}\text{Mn}_y\text{Te}$ QW in a stripe geometry with width L_y (x direction is infinite). The key feature of finite size effect is the gap opening in the energy dispersion of the edge states, resulted from their mutual coupling. In Fig. 1, we plot the energy spectrum of the strip with sample width L_y from 400 nm to 25 nm ($y = 0.02$ and $\langle S\rangle = 1$), where red (blue) line indicates the dispersion of the up (down) spin edge states. In Fig. 1(a), the sample width is 400 nm. The L_y is large enough, so that there is no coupling between edge states. We can see that the dispersion of edge states is gapless for both up and down spin. The sample is in the QSH regime, the charge conductance is $2e^2/h$ and robust against disorder.²⁹ Note that here the QSH state is TRS broken due to the magnetic doping³⁰. Decreasing the width to 200 nm, see Fig. 1(b), the coupling between the down spin edge states is strong enough to open a measurable gap, while the up spin states remain gapless. As a result, charge conduction through the down spin edge channels is no longer topological protected, and backscattering by impurity becomes possible. Hence, with some disorder, the charge conductance in this regime should range from $2e^2/h$ to e^2/h . A typical case is that, when the Fermi level is in the energy gap of down spin states,

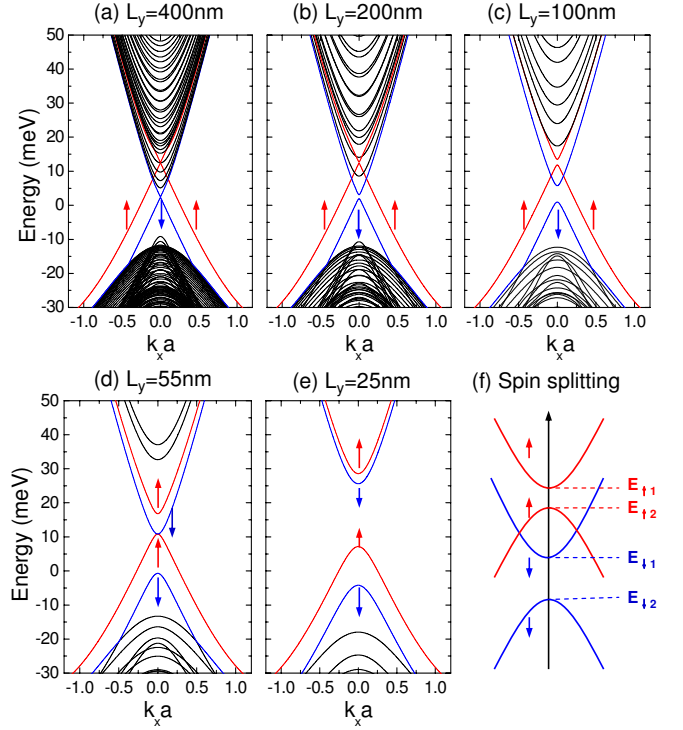


FIG. 1: (Color online) The band structure and edge states upon decreasing the $\text{Hg}_{(1-y)}\text{Mn}_y\text{Te}$ width L_y for the Mn doping $y = 0.02$ and the Mn spin polarization $\langle S\rangle=1$ in the figures (a)-(e). In the figure (f), we illustrate the definition of $E_{1\uparrow}$ ($E_{1\downarrow}$) and $E_{2\uparrow}$ ($E_{2\downarrow}$), which are the energies of two spin-up (spin-down) edge bands at the zero momentum points. The definition is useful for following discussions

the charge conductance becomes e^2/h and the transport property is now similar as that of the QAH state. So we call this transport regime as QAH regime. But it should be emphasized that the QAH transport regime here results from the finite size effect, different from the normal conception of QAH state. In Fig. 1(c), when the sample width L_y is decreased to 100 nm, all the edge states become gapped. Meanwhile, due to the spin splitting, near the $k_x = 0$ point, the down band of spin up is higher than the up band of spin down. No matter where the Fermi level is (still in the bulk gap), there are always conducting edge channels near the Fermi level. This is the edge conducting regime, in which conduction through the edge can be completely killed by disorder. The conductance can range from $2e^2/h$ to 0. Decreasing L_y further, the energy gaps increase and we get a normal insulator, see Fig. 1(d) and (e). From above results, we see that the coupling between edge states in the QAH system is spin dependent. This is not surprising, because the two spin blocks in the Hamiltonian [Eq. (1)] are no longer related by TRS, due to magnetic doping. A direct consequence is that there are four kinds of transport regime: QSH regime, QAH regime, edge conducting (EC) regime and normal insulator (NI) regime.

To illustrate the above physical picture more clearly,

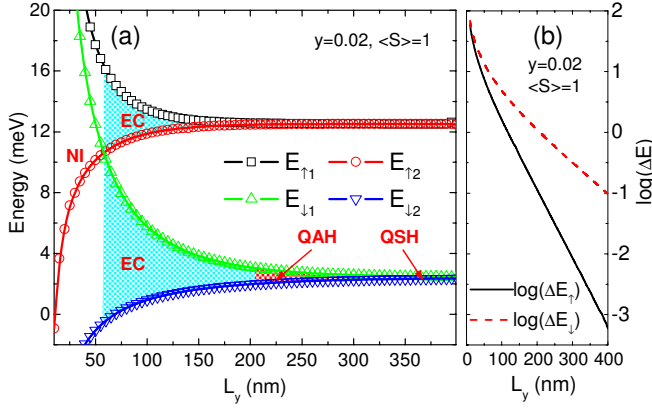


FIG. 2: (Color online) (a) The band energies $E_{1\uparrow}$, $E_{2\uparrow}$, $E_{1\downarrow}$ and $E_{2\downarrow}$ as a function of QW width L_y , with the Mn spin polarization $\langle S \rangle = 1$ and the doping $y = 0.02$. The transport regimes are shown as well. (b) The energy gaps $\log(\Delta E_{\uparrow})$ and $\log(\Delta E_{\downarrow})$, where $\Delta E_{\uparrow} = (E_{1\uparrow} - E_{2\uparrow})$ and $\Delta E_{\downarrow} = (E_{1\downarrow} - E_{2\downarrow})$.

with the same parameters as Fig. 1, we plot the energy of the edge states at $k_x = 0$, namely $E_{1\uparrow}$, $E_{1\downarrow}$, $E_{2\uparrow}$ and $E_{2\downarrow}$ shown in Fig. 1(f), as a function of sample width L_y in Fig. 2 (a). When L_y is large, the up and down bands for spin up (down) touche at $k_x = 0$. All the edge bands are gapless and it is in QSH regime. Decreasing the width, we can see that a measurable gap (larger than 0.1 meV) appears for the down spin, but the up spin is still gapless. In this QAH regime, the transport behavior is the same as the QAH state. Decreasing further, we enter the EC regime, where all the edge bands are gapped and the up band of spin down is lower than the down band of spin up. In this regime, we always have EC channels with insulating bulk. But the conductance of EC could be completely destroyed by disorder. When the up band of spin down touches the down band of spin up, we get a critical point which separates the EC regime from the NI regime [see Fig. 1(d)]. In NI regime, the system is insulating for both bulk and edges. In Fig. 2(b), we show that, for both spin up and down, the gap decays exponentially as a function of width L_y , if L_y is not too small.

Given the width of the HgMnTe QW sample, different doping situation will give different transport behaviour. As shown above, the magnetic doping in our model is described by the spin splitting, which is determined by the product of doping concentration y and local spin polarization $\langle S \rangle$. Take $L_y = 150\text{nm}$ as example, we illustrate the variation of the transport regime when changing the doping situation. Here, we set $y = 0.02$ and change the value of $\langle S \rangle$. We calculate the energy of edge bands, as well as the gap, for both spin up and down as a function of $\langle S \rangle$. The results are shown in Fig. 3(a) and (b). With similar analysis, increasing the spin polarization, we can see that the system will evolve from the NI regime [Fig. 3(c)] into the EC regime [Fig. 3(d)] and finally into the QAH regime [Fig. 3(e)]. Nevertheless, the difference

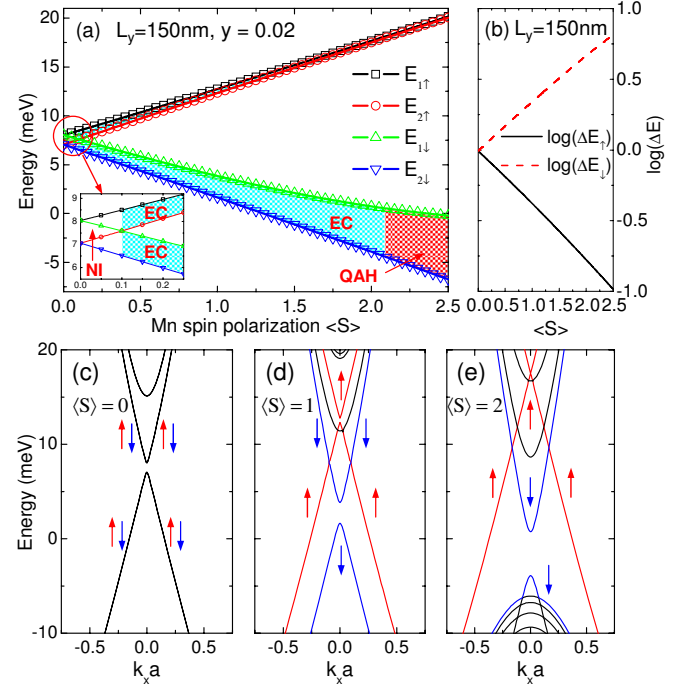


FIG. 3: (Color online) (a) The band energies $E_{1\uparrow}$, $E_{2\uparrow}$, $E_{1\downarrow}$ and $E_{2\downarrow}$ as a function of the Mn spin polarization $\langle S \rangle$ with $L_y = 150\text{nm}$ and the Mn doping $y = 0.02$. The transport regimes are shown as well. (b) The corresponding energy gaps $\log(\Delta E_{\uparrow, \downarrow})$. (c)-(e) The energy spectra of three chosen structures with different values of $\langle S \rangle$.

from the case of changing sample width (see Fig. 2) is that, increasing the spin polarization, the energy gap for down spin decays exponentially, while the gap for up spin is just opposite, as shown in Fig. 3(b). This implies that for a narrow HgMnTe sample in the NI regime, enhancing the Mn spin polarization is still an effective route to realize QAH effect.

Now we study the whole diagram of the transport regime with three tunable parameters: sample width L_y , spin polarization $\langle S \rangle$ and Mn doping concentration y . In Fig. 4 (a) and (b), the gap of edge states for up spin and down spin is plotted in L_y - $\langle S \rangle$ plane, respectively. The results in L_y - y plan are plotted in Fig. 4(c) and (d). Figure 4 summarizes the central result of this paper, where white lines represent boundaries between different regimes. We assume that only the gap larger than 0.1 meV can be detected in transport experiment, which is used as a criteria of the gap opening. At zero $\langle S \rangle$ (or $y = 0$) limit, the problem is reduced to the finite size effect of QSH system, and our results are well consistent with previous work.¹⁷ An important feature is that the finite size effect can fundamentally change the transport character. With the same spin polarization, each transport regime has its own permitted width range. For example, if one wants to get only one quantized conducting channel, i.e. the QAH transport regime, the width of sample should be in the range from 160 nm to 280 nm

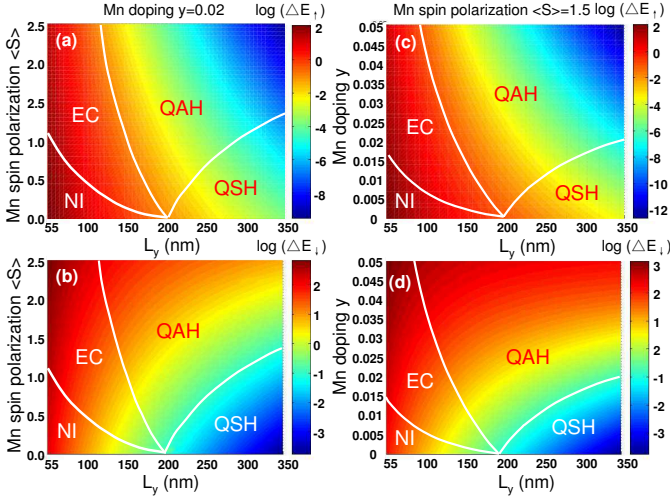


FIG. 4: (Color online) Phase diagram in the $(\langle S \rangle, L_y)$ plane for the Mn doping $y = 0.02$ is shown in the figures (a) and (b), and the phase diagram in the (y, L_y) plane for the Mn spin polarization $\langle S \rangle = 1.5$ is shown in the figures (c) and (d). In the all figures, the energy gaps for the up spins and down spins ($\log(\Delta E_\uparrow)$ and $\log(\Delta E_\downarrow)$) are plotted, where four kinds of transport regimes, i.e., QSH regime, QAH regime, EC regime and NI regime, are shown.

when $\langle S \rangle = 1$ and $y = 0.02$. The permitted width range for the transport regime is important for the device application because that one has to choose proper device width to get the right transport property. Meanwhile, it is also important for the nanomaterials with QAH phase since the coupling between edge states normally can not be ignored in these materials. Another important conclusion is that the minimal spin polarization (or doping concentration), required to obtain the QAH transport regime, depends on the sample width, which is small in moderate width region.

In summary, we numerically study the finite size effect in QAH system using HgMnTe QW as an example. We demonstrate that the coupling of edge states in QAH system depends on both the sample width and the magnetic doping. Thus, choosing proper sample width and doping, we get four different transport regimes, each of which

has fundamentally different transport properties. (1) In QSH regime, there are two quantized conducting channel near the edge which are robust against disorder. There is no coupling between edge states. The charge conductance is $2e^2/h$. (2) In QAH regime, the coupling between the edge states of down spin becomes strong enough to open an observable gap, while the edge bands of up spin is still gapless. The coupling makes the backscattering by disorder possible in down spin edge conducting channel. Hence, in this regime there is only one topological protected conducting channel left and the charge conductance ranges from $2e^2/h$ to e^2/h , depending on the disorder and position of Fermi level. (3) In EC regime, no matter where the Fermi level is, there are always edge states near the Fermi level. But due to the gap opening, all the edge conducting channels can be destroyed by disorder. So the charge conductance is in the region between $2e^2/h$ and zero, the value of which is also determined by the disorder and the position of Fermi level. (4) In NI regime, it is insulating in both bulk and edge. We give the whole diagram of the transport regime in QAH system. For each regime, the permitted width region and the corresponding doping region required are clearly shown in the diagram. An interesting result is that the moderate width region is favored to get the QAH transport regime. The transport property in QAH system is very important, because it is not only of fundamentally importance but also is the basis of future device applications. The quantized conductance is the key feature of the topological nontrivial phase. Meanwhile, novel quantum electronic device will also base on the transport property. Our results give the relation among the sample width, magnetic doping and the transport property. It will be useful for the analysis and design of the transport experiments in QAH systems.

This work was supported by the National Natural Science Foundation of China (Nos. 11274128, 11074081 and 10804034). J.H.G acknowledges support from the National Natural Science Foundation of China (Grants No. 11274129). J.T.L. acknowledges from the National Natural Science Foundation of China (Grants No. 11304107 and No. 61371015), and the Fundamental Research Funds for the Central Universities (HUST:2013TS032).

* Electronic address: hhfu@mail.hust.edu.cn

† Electronic address: jinhua@mail.hust.edu.cn

¹ J. Wang, B. Lian, H. Zhang, Y. Xu, and S.-C. Zhang, Phys. Rev. Lett. **111**, 136801 (2013).

² J. Wang, B. Lian, H. Zhang, and S.-C. Zhang, Phys. Rev. Lett. **111**, 086803 (2013).

³ H.-Z. Lu, A. Zhao, and S.-Q. Shen, Phys. Rev. Lett. **111**, 146802 (2013).

⁴ X. Liu, H.-C. Hsu, and C.-X. Liu, Phys. Rev. Lett. **111**, 086802 (2013).

⁵ C.-X. Liu, X.-L. Qi, X. Dai, Z. Fang, and S.-C. Zhang, Phys. Rev. Lett. **101**, 146802 (2008).

⁶ M. Onoda and N. Nagaosa, Phys. Rev. Lett. **90**, 206601 (2003).

⁷ X.-L. Qi, Y.-S. Wu, and S.-C. Zhang, Phys. Rev. B **74**, 085308 (2006).

⁸ X.-L. Qi, T.L. Hughes, and S.-C. Zhang, Phys. Rev. B **78**, 195424 (2008).

⁹ R. Li, J. Wang, X.-L. Qi, and S.-C. Zhang, Nat. Phys. **6**, 284 (2010).

¹⁰ R. Yu, W. Zhang, H.-J. Zhang, S.-C. Zhang, X. Dai, and Z. Fang, Science **329**, 61 (2010).

¹¹ F. D. M. Haldane, Phys. Rev. Lett. **61**, 2015 (1988).

¹² X. L. Qi and S. C. Zhang, Phys. Today **63**(1), 33 (2010).

- ¹³ Z. Qiao, S. A. Yang, W. Feng, W.-K. Tse, J. Ding, Y. Yao, J. Wang, and Q. Niu, Phys. Rev. B **82**, 161414(R) (2010).
- ¹⁴ J. Ding, Z. H. Qiao, W. X. Feng, Y. G. Yao, and Q. Niu, Phys. Rev. B **84**, 195444 (2011).
- ¹⁵ M. Ezawa, Phys. Rev. Lett. **109**, 055502 (2012).
- ¹⁶ C.-Z. Chang, J. Zhang, X. Feng, J. Shen, Z. Zhang, M. Guo, K. Li, Y. Ou, P. Wei, L.-L. Wang, Z.-Q. Ji, Y. Feng, S. Ji, X. Chen, J. Jia, X. Dai, Z. Fang, S.-C. Zhang, K. He, Y. Wang, L. Lu, X.-C. Ma, and Q.-K. Xue, Science **340**, 167 (2013).
- ¹⁷ B. Zhou, H.-Z. Lu, R.-L. Chu, S.Q. Shen, and Q. Niu, Phys. Rev. Lett. **101**, 246807 (2008).
- ¹⁸ J. Linder, T. Yokoyama T, and A. Sudbø, Phys. Rev. B **80**, 205401 (2009).
- ¹⁹ H. Z. Lu, W. Y. Shan, W. Niu, and S. Q. Shen, Phys. Rev. B **81**, 115407 (2010).
- ²⁰ B. A. Bernevig, T. L. Hughes and S. C. Zhang, Science **314**, 1757-1761 (2006).
- ²¹ M. König *et al.*, Science **318**, 766 (2007).
- ²² W. Beugeling, C. X. Liu, E. G. Novik, L. W. Molenkamp, and C. Morais Smith, Phys. Rev. B **85**, 195304 (2012).
- ²³ B. Buttner, C. Liu, G. Tkachov, E. Novik, C. Bruene, H. Buhmann, E. Hankiewicz, P. Recher, B. Trauzettel, S.-C. Zhang, and L. W. Molenkamp, Nat. Phys. **7**, 418 (2011).
- ²⁴ J. Li, R. L. Chu, J. K. Jain, and S. Q. Shen, Phys. Rev. Lett. **102**, 136806 (2009).
- ²⁵ H. Jiang, L. Wang, Q.-F. Sun, and X. C. Xie, Phys. Rev. B **80**, 165316 (2009).
- ²⁶ Y. Xing, L. Zhang, and J. Wang, Phys. Rev. B **84**, 035110 (2011).
- ²⁷ J. K. Furdyna, J. Appl. Phys. **64**, R29 (1988).
- ²⁸ E. G. Novik, Phys. Rev. B **72**, 035321 (2005).
- ²⁹ Y. Xing, L. Zhang, and J. Wang, Phys. Rev. B **84**, 035110 (2011).
- ³⁰ Yunyou Yang, Zhong Xu, L. Sheng, Baigeng Wang, D. Y. Xing, and D. N. Sheng, Phys. Rev. Lett. **107**, 066602 (2011).